

R 50 as a beam quality specifier for selecting stopping-power ratios and reference depths for electron dosimetry

D. T. Burns, G. X. Ding, and D. W. O. Rogers

Citation: *Medical Physics* **23**, 383 (1996); doi: 10.1118/1.597893

View online: <http://dx.doi.org/10.1118/1.597893>

View Table of Contents: <http://scitation.aip.org/content/aapm/journal/medphys/23/3?ver=pdfcov>

Published by the American Association of Physicists in Medicine

Articles you may be interested in

[Prediction of stopping-power ratios in flattening-filter free beams](#)

Med. Phys. **37**, 1164 (2010); 10.1118/1.3314074

[Accuracy of the Burns equation for stopping-power ratio as a function of depth and R 50](#)

Med. Phys. **31**, 2961 (2004); 10.1118/1.1803811

[Effects of changes in stopping-power ratios with field size on electron beam relative output factors](#)

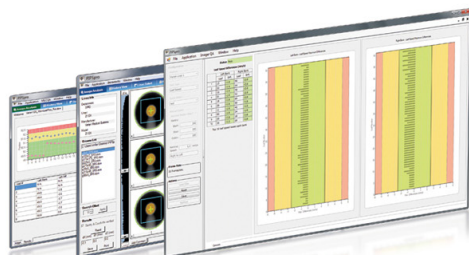
Med. Phys. **25**, 1711 (1998); 10.1118/1.598351

[Calculation of stopping-power ratios using realistic clinical electron beams](#)

Med. Phys. **22**, 489 (1995); 10.1118/1.597581

[On the selection of stopping-power and mass energy-absorption coefficient ratios for high-energy x-ray dosimetry](#)

Med. Phys. **11**, 618 (1984); 10.1118/1.595643



PIPSPRO SOFTWARE
NEW VERSION 5.2

True Quantitative Leaf Speed Loss,
Not Just Qualitative Results

Click to Learn More


www.standardimaging.com | 608-831-0025

R_{50} as a beam quality specifier for selecting stopping-power ratios and reference depths for electron dosimetry

D. T. Burns

Centre for Ionising Radiation and Acoustics, National Physical Laboratory, Teddington, Middlesex, UK TW11 0LW

G. X. Ding and D. W. O. Rogers^{a)}

Ionizing Radiation Standards, Institute for National Measurement Standards, National Research Council Canada, Ottawa, Canada K1A 0R6

(Received 23 June 1995; accepted for publication 27 December 1995)

For electron beam reference dosimetry in radiotherapy, it is shown that by choosing the reference depth as $d_{\text{ref}} = 0.6R_{50} - 0.1$ cm, where R_{50} is the half-value depth in centimeters, the Spencer–Attix water-to-air stopping-power ratio at d_{ref} is given by $(\bar{L}/\rho)_{\text{air}}^w = 1.2534 - 0.1487 (R_{50})^{0.2144}$. This is derived from data for $(\bar{L}/\rho)_{\text{air}}^w$ obtained from realistic Monte Carlo simulations for 24 clinical beams. The rms deviation of this expression from the Monte Carlo calculations is 0.16%, with a maximum deviation of 0.26%. This approach fully takes into account the spectral differences between real electron beams of the same R_{50} and allows an absorbed-dose calibration at a standards laboratory to be easily and accurately transferred to a reference clinical beam. Using a single parameter to specify $(\bar{L}/\rho)_{\text{air}}^w$, rather than the two parameters (R_{50} and depth) needed when the reference depth is chosen as the depth of dose maximum, has the potential to greatly simplify electron beam dosimetry protocols and allows the use of a similar formalism for photon and electron beam dosimetry. For use in converting a depth–ionization curve into a depth–dose curve, a somewhat less accurate but general expression for $(\bar{L}/\rho)_{\text{air}}^w$ as a function of R_{50} and depth is presented.

87.53.03

I. INTRODUCTION

When an ion chamber is used for dosimetry in radiotherapy electron beams, its response per unit absorbed dose in a water phantom varies with beam quality and measurement depth. This variation is determined mainly by the Spencer–Attix water-to-air stopping-power ratio at the chosen point of measurement, $(\bar{L}/\rho)_{\text{air}}^w$. For accurate reference dosimetry using a calibrated ion chamber one must therefore specify the beam quality and the reference depth in water in a manner which allows an accurate transfer of $(\bar{L}/\rho)_{\text{air}}^w$.

The approach used in most protocols (for example the AAPM's TG-21 protocol¹ or the IAEA Code of Practice²) is first to determine the mean electron energy at the phantom surface, \bar{E}_0 , using a given relationship between this energy and the half-value depth, R_{50} . The chamber is then positioned at a specified reference depth, d_{ref} , in water and the value of $(\bar{L}/\rho)_{\text{air}}^w$ at d_{ref} is determined from tables which give $(\bar{L}/\rho)_{\text{air}}^w$ as a function of \bar{E}_0 and depth in water. Note that throughout this paper, R_{50} is defined as the half-value of the depth–dose distribution, not the depth–ionization distribution from an ion chamber, for a nominal source-to-surface distance of 100 cm and a broad beam. The conversion between depth–ionization and depth–dose involves a small correction to the half-value which is easily evaluated, at least for an ideal ion chamber.³

In the current protocols the reference depth is normally chosen as the depth of the absorbed-dose maximum, d_{max} , or a specified depth which is deeper than d_{max} . This is problematic in that at incident energies above 10 MeV the value of d_{max} can vary by a large amount from machine to machine for beams of the same R_{50} . It follows that the value of $(\bar{L}/\rho)_{\text{air}}^w$ at d_{max} will also vary between machines for beams

of the same R_{50} . This leads to the need to express $(\bar{L}/\rho)_{\text{air}}^w$ as a function of both R_{50} and depth. Furthermore, the tabulations of $(\bar{L}/\rho)_{\text{air}}^w$ in current protocols are derived from Monte Carlo simulations which use mono-energetic electron beams incident upon the phantom. This is also known to introduce significant errors.^{3–5}

Ding *et al.*³ addressed this latter problem by calculating $(\bar{L}/\rho)_{\text{air}}^w$ as a function of depth for a large number of realistic clinical electron beams simulated using the BEAM code⁶ based on the EGS4 system for Monte Carlo transport.^{7,8} They found that corrections to the mono-energetic calculations of $(\bar{L}/\rho)_{\text{air}}^w$ at d_{max} could be expressed in terms of a simple formula involving the magnitude of the bremsstrahlung tail. The size of the corrections required depends upon the details of the protocol adopted, but the range of corrections is well over 1% for the beams investigated. Although these calculations represent a significant step forward, to utilize this information one must follow a complex procedure in which the mean energy of the electron beam at the phantom surface, \bar{E}_0 , is derived from the measured R_{50} . For this \bar{E}_0 , the value of $(\bar{L}/\rho)_{\text{air}}^w$ at the measured d_{max} is extracted from the tables for mono-energetic beams, and finally the correction to this value of $(\bar{L}/\rho)_{\text{air}}^w$ is determined from a measurement of the size of the bremsstrahlung tail.

This paper proposes a new reference depth, d_{ref} , for electron beam dosimetry, defined simply in terms of the half-value depth R_{50} . It is shown that at this reference depth, the value for the stopping-power ratio $(\bar{L}/\rho)_{\text{air}}^w$ calculated by Ding *et al.*³ for realistic beams can be derived directly from the single parameter R_{50} . The potential impact on dosimetry protocols and on absorbed-dose calibrations of using R_{50} as an electron beam quality specifier is discussed.

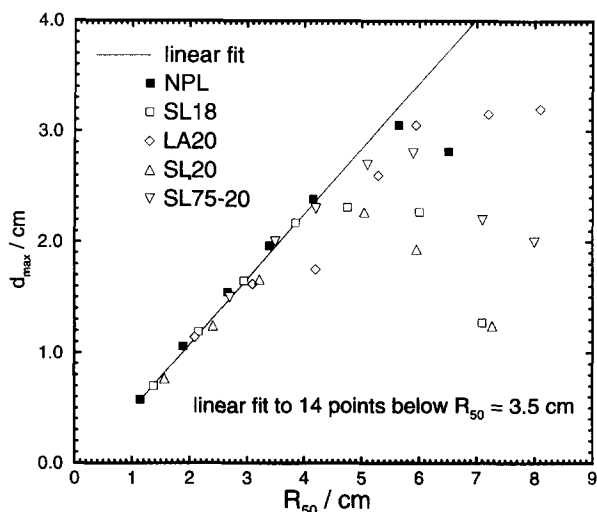


FIG. 1. Location of the depth of dose maximum, d_{\max} , vs R_{50} . The values shown are from experimental measurements on four clinical accelerators and the NPL's research accelerator. The fit is to all beams with $R_{50} < 3.5$ cm.

II. DEPTH OF d_{\max} RELATIVE TO R_{50}

As noted above, one problem with the traditional approach of using d_{\max} as the reference depth is that d_{\max} varies significantly with other characteristics of the beam which do not affect R_{50} . In particular, low-energy electrons scattered into the phantom from the accelerator head raise the surface dose relative to that at depth but do not significantly change R_{50} . At higher incident energies, the dose buildup gradient in a "clean" beam (that is, without a low-energy in-scatter component) becomes shallower as a result of less scattering at these energies. This effect combines with the increased surface dose due to in-scatter to move the position of d_{\max} to shallower depths. The extent of this movement is dependent upon the details of the accelerator head.

Figure 1 shows a plot of measured values of d_{\max} against R_{50} for 27 beams with various energies from four clinical accelerators. Also included are data for seven beams with different energies from the research accelerator of the National Physical Laboratory (NPL), which is very different in design from the clinical machines. It is clear that for values of R_{50} above 4 cm there is a considerable variation in d_{\max} for a given R_{50} . Conversely, the data at lower values of R_{50} form a reasonable straight line. A linear fit to the 14 points with $R_{50} < 3.5$ cm gives

$$d_{\max} = 0.6R_{50} - 0.1 \text{ (cm)} \quad (\text{for } 1.0 < R_{50} < 3.5 \text{ cm}). \quad (1)$$

Figure 2 shows the effect of this variation in d_{\max} on the value of $(\bar{L}/\rho)_{\text{air}}^w$ at d_{\max} , plotted as a function of R_{50} . The data are from the calculations of Ding *et al.*^{3,9} For values of R_{50} in the region of 6 or 7 cm (that is, an incident energy of around 15 MeV) the spread in $(\bar{L}/\rho)_{\text{air}}^w$ is over 3%. By implication, an absorbed-dose calibration made at d_{\max} in the NPL 16-MeV beam could lead to an error of as much as 3% if used at d_{\max} in a clinical beam of the same R_{50} . The situation is somewhat improved in this energy range if one

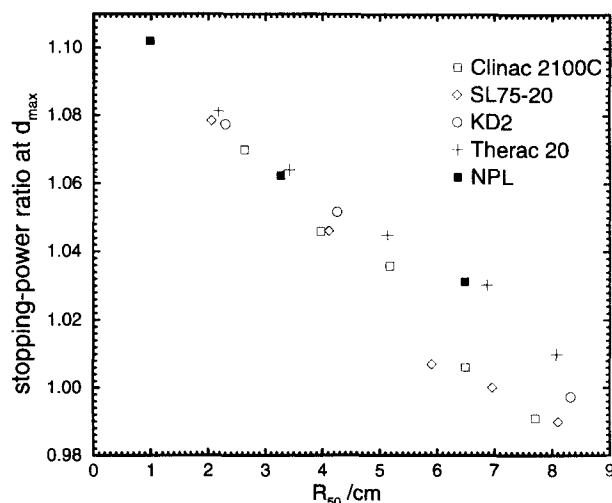


FIG. 2. Variation in Spencer-Attix water-to-air stopping-power ratios at d_{\max} as a function of R_{50} . Data are from Refs. 3 and 9.

takes the reference depth to be at a fixed depth of 1 or 2 cm, as demonstrated in Fig. 3. However, the potential error is still as much as 1%.

III. PROPOSAL FOR A NEW REFERENCE DEPTH

Given the experimentally derived equation (1), one can reanalyze the calculations of Ding *et al.* to study the machine-to-machine variation in $(\bar{L}/\rho)_{\text{air}}^w$ at a new reference depth defined by

$$d_{\text{ref}} = 0.6R_{50} - 0.1 \text{ (cm)} \quad (\text{for } R_{50} \geq 1.0 \text{ cm}). \quad (2)$$

Such a definition of d_{ref} has the advantage of representing d_{\max} at lower energies, where it is important to perform reference dosimetry at the peak, and at higher energies is insensitive to the changing position of d_{\max} for a given R_{50} . It is also a very simple and easily remembered relationship.

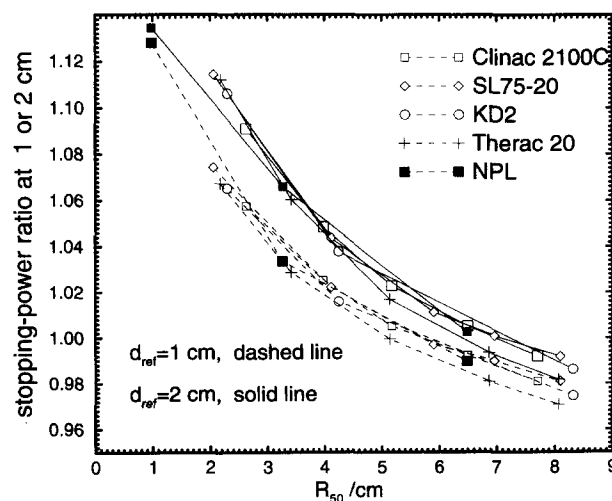


FIG. 3. Variation in stopping-power ratios at fixed depths of 1 or 2 cm as a function of R_{50} . Data based on Refs. 3 and 9.

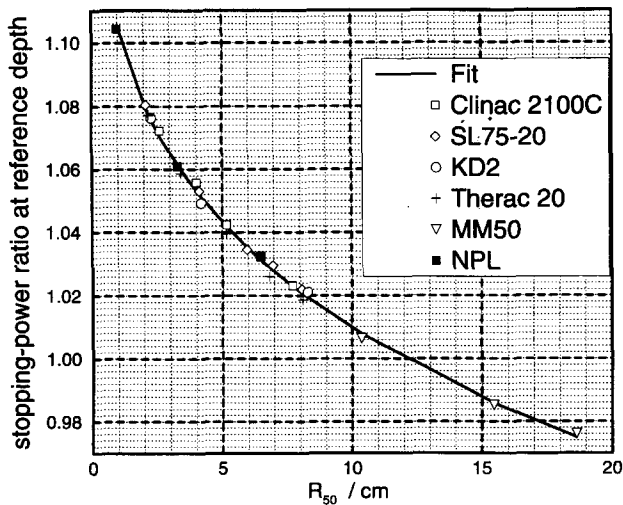


FIG. 4. Fit of $(\bar{L}/\rho)_{\text{air}}^w$ at the reference depth to $a + bR_{50}^c$ for $d_{\text{ref}} = 0.6R_{50} - 0.1$ (cm). The rms deviation is 0.16% and the maximum deviation is 0.26%. The stopping-power ratios and R_{50} values are those calculated for realistic beams by Ding *et al.* (Refs. 3 and 9).

The analysis was performed by first extracting from the work of Ding *et al.* the value of $(\bar{L}/\rho)_{\text{air}}^w$ at this d_{ref} for each of the 24 beams calculated. These data are plotted in Fig. 4 and show a smooth curve with little machine-to-machine variation. This is a somewhat unexpected though welcome finding and forms the basis of the new proposal. The data at this d_{ref} are fitted to an equation of the form

$$\left(\frac{\bar{L}}{\rho}\right)_{\text{air}}^w(R_{50}) = a + b(R_{50})^c, \quad (3)$$

where, for the particular choice of d_{ref} given by Eq. (2), a least squares fit gives the values $a = 1.2534$, $b = -0.1487$, and $c = 0.2144$. The rms deviation of the data about this fit is 0.16% with a maximum deviation of 0.26%. This result shows that for this choice of reference depth the water-to-air stopping-power ratio, $(\bar{L}/\rho)_{\text{air}}^w$, is well defined by the single beam quality specifier R_{50} . This equation is expected to be very robust for all clinical electron beams used for reference dosimetry since the set of beams studied ranged from virtually mono-energetic scanned beams to those with broad energy spectra from single scattering foil machines (see Ref. 10).

The uniqueness of the particular choice of d_{ref} given by Eq. (2) was studied by performing the same analysis at a series of reference depths defined by $0.1R_{50}$, $0.2R_{50}$, etc., up to the value $1.5R_{50}$. The best fit is at the depth defined by $0.7R_{50}$ (rms deviation 0.10% and maximum deviation 0.18%). However, this depth is not preferable to that defined by Eq. (2) because at low energies $0.7R_{50}$ is beyond d_{max} and so the dose gradient is much steeper. This is shown clearly in Fig. 5, which plots the dose gradient (in % per mm) for each of the 24 beams at the depths $0.7R_{50}$ and $0.6R_{50} - 0.1$. For R_{50} down to 1 cm the gradient at $0.7R_{50}$ can be up to -10% per mm whereas at $0.6R_{50} - 0.1$ it is around -1% per mm or less. Since there is some uncertainty associated with correc-

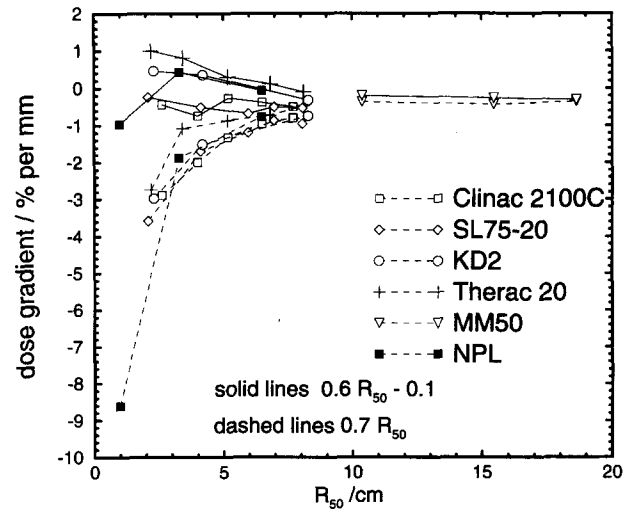


FIG. 5. Calculated dose gradient, i.e., percentage change in the dose per millimeter for the 1-mm region (± 0.5 mm) about depths of $0.7R_{50}$ and $0.6R_{50} - 0.1$. Values are from calculated depth-dose curves (Refs. 6 and 10) and are only indicative.

tions related to the gradient, it is best to minimize the gradient at the reference depth (see discussion below in Sec. IV C).

IV. DISCUSSION

A. Impact on electron beam absorbed-dose calibrations

One of the principle drives behind the search for an improved beam quality specifier was to maximize the absorbed-dose transfer accuracy for the proposed NPL electron beam calibration service.¹¹ The NPL proposal is to calibrate user reference chambers in terms of water absorbed dose at a series of qualities specified in terms of R_{50} , with d_{ref} at each R_{50} given according to Eq. (2). Thus the absorbed-dose calibration factor $N_{D,w}$ for an ion chamber can be specified solely as a function of R_{50} . Since this is a smoothly varying function, it is easy to interpolate between the NPL calibration qualities and the user reference qualities. It is evident from Fig. 4 that the transfer of the calibration from NPL to the clinic will not introduce an error of more than 0.3%, typically less than 0.2%, which is negligible in terms of the overall uncertainty.

The shape of Fig. 4 represents the approximate shape of the calibration curve for $N_{D,w}$. The actual curve for $N_{D,w}$ will be modified by the perturbation caused by the presence of the chamber. The calibration factor at d_{ref} in a beam with quality R'_{50} can be derived from that at quality R_{50} according to

$$N_{D,w}(R'_{50}) = N_{D,w}(R_{50}) \frac{\left[P_{\text{wall}} P_{\text{repl}} \left(\frac{\bar{L}}{\rho} \right)_{\text{air}}^w \right]_{R'_{50}}}{\left[P_{\text{wall}} P_{\text{repl}} \left(\frac{\bar{L}}{\rho} \right)_{\text{air}}^w \right]_{R_{50}}} \quad (\text{Gy/C}). \quad (4)$$

The stopping-power terms are easily evaluated from Eq. (3). The perturbation factors P_{wall} and P_{repl} correct for the non-medium equivalence of the chamber materials and cavity and are fully discussed in Ref. 12. The measurement at a standards laboratory of $N_{D,w}$ at the new d_{ref} as a function of R_{50} will give high-quality data on the variation of $P_{\text{wall}}P_{\text{repl}}$ with R_{50} . These data can then be applied to an arbitrary clinical beam using Eq. (4). By implication, the end result may be that only a single electron beam calibration factor is required.

Note that this approach assumes that at the new reference depth, d_{ref} , the combined factor $P_{\text{wall}}P_{\text{repl}}$ for a given chamber can also be well specified by R_{50} . Although this has not been demonstrated, it is plausible and, in any event, its variation with energy is much slower than that for $(\bar{L}/\rho)_{\text{air}}^w$ so that no major uncertainty should be introduced.

B. Impact on the k_Q formalism using ^{60}Co absorbed-dose calibrations

Another major drive behind the search for an improved beam quality specifier is to allow the development of a protocol formalism for electron beams which parallels the k_Q formalism for photon beams.¹³⁻¹⁵ The k_Q approach starts from an absorbed-dose calibration factor rather than an air-kerma calibration factor. This leads to a simple formalism in which the absorbed dose to water at the reference depth in water is derived according to

$$D_w^Q = M k_Q N_{D,w}^{60\text{Co}} \text{ (Gy)}, \quad (5)$$

where M is the corrected chamber reading, $N_{D,w}^{60\text{Co}}$ is the water absorbed-dose calibration factor for the chamber in ^{60}Co radiation, and k_Q converts the ^{60}Co calibration factor to a calibration factor for a beam of quality Q . The main application of this formalism has been in photon dosimetry, where beam qualities are generally expressed in terms of a single beam quality parameter. A significant drawback in using this formalism for electron dosimetry has been the need to use two parameters to specify beam quality, \bar{E}_0 and d_{max} .

By using the single electron beam quality specifier R_{50} , k_Q can be written as

$$k_Q = k_{R_{50}} = \frac{\left[P_{\text{wall}} P_{\text{repl}} \left(\frac{\bar{L}}{\rho} \right)_{\text{air}}^w \right]_{R_{50}}}{\left[P_{\text{wall}} P_{\text{repl}} \left(\frac{\bar{L}}{\rho} \right)_{\text{air}}^w \right]_{^{60}\text{Co}}}, \quad (6)$$

where $(\bar{L}/\rho)_{\text{air}}^w(R_{50})$ is given by Eq. (3). Therefore the new approach provides a formalism which is identical for photon and electron beams. However, if using calculated values, the advantage of using $k_{R_{50}}$ in electron beams is not so great as using k_Q in photon beams since $k_{R_{50}}$ requires the evaluation of ratios of $P_{\text{wall}}P_{\text{repl}}$ factors in electron and photon beams where these parameters are conceptually different, whereas k_Q only requires ratios of $P_{\text{wall}}P_{\text{repl}}$ in photon beams at dif-

ferent energies.¹⁴ If measured values of $k_{R_{50}}$ for a given chamber type are used, then the full advantage of this formalism is obtained.

Alternatively, where the standards are available, the reference radiation could be taken to be an electron beam quality rather than ^{60}Co radiation. This has the advantage of requiring only ratios of $P_{\text{wall}}P_{\text{repl}}$ in electron beams at different beams at different energies as derived by Eq. (4).

C. Potential problems when d_{ref} is not at d_{max}

At higher energies the reference depth given by Eq. (2) is generally deeper than d_{max} , which is potentially a problem for the correction factor P_{repl} at these energies. As discussed in Ref. 12 this correction is a product of two factors, a fluence correction factor P_{fl} and a gradient correction factor P_{gr} . For cylindrical ion chambers the fluence correction factor P_{fl} at d_{max} can be several percent at higher energies. To the extent to which P_{fl} varies with depth, its value at the new reference depth d_{ref} is not currently known.

A second problem, specific to protocols which do not use an effective point of measurement (e.g., the AAPM TG-21 protocol¹), is that the gradient correction factor P_{gr} at the new reference depth cannot be assumed to be unity as it is at d_{max} . This problem is dealt with (for example by the HPA¹⁶ and IAEA²) by assuming the effective point of measurement to be a specified distance in front of the central axis and by positioning the chamber accordingly. However, the exact location of the effective point of measurement is not precisely known and there is an advantage in minimizing the dose gradient at the reference depth. As discussed above and demonstrated by Fig. 5, this is another reason for preferring Eq. (2) for the reference depth over a reference depth specified as $0.7R_{50}$.

These problems are minimized if parallel-plate ion chambers are used for electron dosimetry. The P_{gr} correction for parallel-plate chambers is accounted for in all protocols by taking the effective point of measurement to be the inside of the front wall of the chamber. The P_{fl} correction is generally taken to be unity for a well-guarded parallel-plate chamber, although there are commercial chambers which are not adequately guarded.¹⁷ Strictly, P_{fl} for such chambers needs to be remeasured at the new reference depth, d_{ref} . However, at the lower energies where this effect may be significant, d_{ref} is very close to d_{max} and the existing data at d_{max} should suffice.¹⁷

The measurement of $P_{\text{repl}} = P_{\text{fl}}P_{\text{gr}}$ for a cylindrical chamber is in principle straightforward, by comparison with a well-guarded parallel-plate chamber (see, for example, Ref. 18), and it is expected that such measurements will be carried out at the new d_{ref} once the potential advantages of the new approach are recognized. However, there is some evidence that even for a well-guarded parallel-plate chamber P_{fl} may not be as close to unity as is generally assumed.¹⁹ Furthermore, there is mounting evidence that the usual assumption that P_{wall} for parallel-plate chambers is unity does not take adequate account of backscatter from the rear chamber wall.^{20,21} All of the above problems are overcome if the

method outlined in Sec. IV A is used to measure the variation in the product $P_{\text{wall}}P_{\text{repl}}$ at d_{ref} as a function of R_{50} .

D. Integration with measurements of depth-dose curves

The use of the methods and data presented here to determine the absorbed dose to water at the reference depth imposes an explicit dependence on the stopping-power ratios calculated by Ding *et al.*³ for realistic electron beams. Thus for consistency one must also use these data to derive the stopping-power ratio at other depths when converting a measured depth-ionization distribution to a depth-dose distribution. To facilitate this, a universal fit to the data of Ding *et al.* is presented, giving an expression for the stopping-power ratio as a function of R_{50} and depth.

Ding *et al.*³ presented calculated stopping-power ratios $(\bar{L}/\rho)_{\text{air}}^w$ as a function of depth z for 21 realistic electron beams and Ding and Rogers⁹ performed similar calculations for 3 of the NPL calibration beams. For the present fit, each of these 24 beams is characterized by the calculated half-value depth R_{50} and stopping-power data are generated for each as a function of z/R_{50} . The R_{50} values range from 0.98–18.6 cm. Discrete values for z/R_{50} range from 0.02–1.2.

The data in this form are fitted by the 3-D version of the Tablecurve software supplied by Jandel Scientific. The best least squares fit to the data is obtained with an equation of the form

$$\left(\frac{\bar{L}}{\rho}\right)_{\text{air}}^w(R_{50}, z) = \frac{a + b(\ln R_{50}) + c(\ln R_{50})^2 + d(z/R_{50})}{1 + e(\ln R_{50}) + f(\ln R_{50})^2 + g(\ln R_{50})^3 + h(z/R_{50})} \quad (7)$$

The values for the eight coefficients given below result in an rms deviation of 0.4% and a maximum deviation of 1.0% for z/R_{50} ranging between 0.02 and 1.1. The maximum deviation is increased to 1.7% if z/R_{50} values up to 1.2 are considered:

$$\begin{aligned} a &= 1.0752 & b &= -0.50867 & c &= 0.088670 \\ d &= -0.08402 & e &= -0.42806 & f &= 0.064627 \\ g &= 0.003085 & h &= -0.12460 \end{aligned}$$

This universal fit can be compared with the best fit for $(\bar{L}/\rho)_{\text{air}}^w$ at the reference depth d_{ref} by putting $z=0.6R_{50}-0.1$ cm into the above equation. This comparison shows that the two fits agree to within 0.1% for R_{50} in the range 3–20 cm, but the discrepancy rises below this range and reaches a maximum value of 0.3% for R_{50} around 1.5 cm. This is not a serious problem but it should be stressed that the universal fit is best applied to relative calculations and in particular to the conversion of a measured depth-ionization distribution into a depth-dose distribution (which also requires taking into account any changes in other factors such as P_{wall} and P_{repl}). For the best determination of the stopping-power ratio at the reference depth, Eq. (3) should be used. [The raw data for

this evaluation and a FORTRAN subroutine for interpolating the data and another for evaluating Eq. (7) are available on the WWW at <http://www.irs.inms.nrc.ca/inms/irs/papers/SPRR50/sprR50.html>.]

V. CONCLUSIONS

The ability to specify the reference depth, d_{ref} , and the water-to-air stopping-power ratio at this depth, $(\bar{L}/\rho)_{\text{air}}^w$, in terms of the single electron beam quality parameter R_{50} , could have a significant impact on reference electron dosimetry. From the point of view of absorbed-dose calibrations at a standards laboratory, the simple and largely machine-independent relationships given by Eqs. (2) and (3) allow such a calibration to be easily transferred to an arbitrary clinical accelerator with no significant increase in the overall uncertainty. In clinical electron dosimetry, these relationships should greatly simplify the procedure by which calibrations are transferred and at the same time yield more consistent dosimetry from center to center. In the longer term this new approach has the potential to rationalize dosimetry protocols such that photon and electron dosimetry are based on a similar formalism.

Another advantage of the new method is that it avoids the need for evaluating \bar{E}_0 , the mean energy at the phantom surface. This quantity has been the subject of much debate and is not completely specified by R_{50} .²² The value of \bar{E}_0 is of no direct relevance to reference dosimetry, although it is of qualitative interest in clinical practice.

^aElectronic-mail: dave@irs.phy.nrc.ca

¹AAPM TG-21, "A protocol for the determination of absorbed dose from high-energy photon and electron beams," Med. Phys. **10**, 741–771 (1983).

²IAEA, International Atomic Energy Agency, "Absorbed Dose Determination in Photon and Electron Beams; An International Code of Practice," Technical Report Series No. 277 (IAEA, Vienna, 1987).

³G. X. Ding, D. W. O. Rogers, and T. R. Mackie, "Calculation of stopping-power ratios using realistic clinical electron beams," Med. Phys. **22**, 489–501 (1995).

⁴P. Andreo, A. Brahme, A. E. Nahum, and O. Mattsson, "Influence of energy and angular spread on stopping-power ratios for electron beams," Phys. Med. Biol. **34**, 751–768 (1989).

⁵P. Andreo and A. Fransson, "Stopping-power ratios and their uncertainties for clinical electron beam dosimetry," Phys. Med. Biol. **34**, 1847–1861 (1989).

⁶D. W. O. Rogers, B. A. Faddegon, G. X. Ding, C.-M. Ma, J. Wei, and T. R. Mackie, "BEAM: A Monte Carlo code to simulate radiotherapy treatment units," Med. Phys. **22**, 503–524 (1995).

⁷W. R. Nelson, H. Hirayama, and D. W. O. Rogers, The EGS4 Code System, Stanford Linear Accelerator Center Report SLAC-265 (Stanford, CA) (1985).

⁸A. F. Bielajew, H. Hirayama, W. R. Nelson, and D. W. O. Rogers, "History, overview and recent improvements of EGS4," National Research Council of Canada Report PIRS-0436 (1994).

⁹G. X. Ding and D. W. O. Rogers, "Monte Carlo simulation of NPL linac and calculation of dose distributions and water/air stopping-power ratios," National Research Council of Canada Report PIRS-0399 (1993).

¹⁰G. X. Ding and D. W. O. Rogers, "Energy spectra, angular spread, and dose distributions of electron beams from various accelerators used in radiotherapy," National Research Council of Canada Report PIRS-0439 (see <http://www.irs.inms.nrc.ca/inms/irs/papers/PIRS439/pirs439.html>) (April, 1995).

¹¹D. T. Burns, M. R. McEwen, and A. J. Williams, "An NPL absorbed dose calibration service for electron beam radiotherapy," IAEA-SM-330/34, in

- Proceedings of Symposium on Measurement Assurance in Dosimetry, (IAEA, Vienna, 1994), pp. 61–71.
- ¹²D. W. O. Rogers, "Fundamentals of High Energy X-ray and Electron Dosimetry Protocols," in *Advances in Radiation Oncology Physics*, edited by J. Purdy, Medical Physics Monograph 19 (AAPM, New York, 1992), pp. 181–223.
 - ¹³K. Hohlfeld, "The standard DIN 6800: Procedures for absorbed dose determination in radiology by the ionization method," in *Dosimetry in Radiotherapy* (Proc. Symp. Vienna, 1987), Vol. 1, pp. 13–24 (1988).
 - ¹⁴D. W. O. Rogers, "The advantages of absorbed-dose calibration factors," *Med. Phys.* **19**, 1227–1239 (1992).
 - ¹⁵P. Andreo, "Absorbed dose beam quality factors for the dosimetry of high-energy photon beams," *Phys. Med. Biol.* **37**, 2189–2211 (1992).
 - ¹⁶HPA, "Code of practice for electron beam dosimetry in radiotherapy," *Phys. Med. Biol.* **30**, 1169–1194 (1985).
 - ¹⁷P. R. Almond, F. H. Attix, S. Goetsch, L. J. Humphries, H. Kubo, R. Nath, and D. W. O. Rogers, "The calibration and use of plane-parallel ionization chambers for dosimetry of electron beams: An extension of the 1983 AAPM protocol, Report of AAPM Radiation Therapy Committee Task Group 39," *Med. Phys.* **21**, 1251–1260 (1994).
 - ¹⁸A. Van der Plaetsen, J. Seuntjens, H. Thierens, and S. Vynckier, "Verification of absorbed doses determined with thimble and parallel-plate ionization chambers in clinical electron beams using ferrous sulphate dosimetry," *Med. Phys.* **21**, 37–44 (1994).
 - ¹⁹C.-M. Ma and A. E. Nahum, "Plane-parallel chambers in electron beams: Monte Carlo findings on perturbation correction factor," in *Proceedings of the IAEA International Symposium on measurement assurance in dosimetry* (IAEA, Vienna, 1994), IAEA-SM-330/71, pp. 481–493.
 - ²⁰M. A. Hunt, G. J. Kutcher, and A. Buffa, "Electron backscatter correction for parallel-plate chambers," *Med. Phys.* **15**, 96–103 (1988).
 - ²¹S. C. Klevenhagen, "Implications of electron backscatter for electron dosimetry," *Phys. Med. Biol.* **36**, 1013–1018 (1991).
 - ²²G. X. Ding, D. W. O. Rogers, and T. R. Mackie, "Mean energy, energy-range relationships and depth-scaling factors for clinical electron beams," *Med. Phys.* **23**, 361–376 (1996).